Sensors & Transducers, Vol. 157, Issue 10, October 2013, pp. 14-19

www.sensorsportal.com

Sensors & Transducers

http://www.sensorsportal.com

Design and Fabricate the High Sensitivity and Stable Optocoupling Sensor

[1] Lei TIAN, [1,2] Xinquan LAI

[1] Institute of Electronic CAD, Xidian University,
Xi'an, Shaanxi 710071, PR China

[2] Key Lab of High-Speed Circuit Design and EMC, Ministry of Education, Xidian University,
Xi'an, Shaanxi 710071, PR China

[1] Tel.: +086-15929907626, fax: 029-88201563
E-mail: tianlei@xupt.edu.cn

Received: 19 August 2013 /Accepted: 25 September 2013 /Published: 31 October 2013

Abstract: A novel photodetector array (PD) and the high sensitivity transimpedance amplifier (TIA) were designed and fabricated for predicting response time based on the optocoupling sensor, implemented in a standard 0.35 μm BCD technology. Based on response time equivalents and the architecture of the optocoupling sensor the response time of the PD were detailed analyzed. The circuit structure and the adjustable gain theory of the TIA module was clarified detailed. At a wavelength of 840 nm, from -25 °C to 125 °C, the simulation results showed that the PD has a high-speed and stable capability. The test results confirm the response time of the whole sensor is 205 ns and 153 ns and the response time would not change with the variation of the temperature. *Copyright © 2013 IFSA.*

Keywords: Optocoupling, Photodetector, Response time, Stability, Sensitivity.

1. Introduction

Nowadays, optocoupling sensor provides an effective means for the electrical isolation between the microelectronic signals [1, 2]. It is widely used in military and aerospace requirements of high reliability field advantages of small size, long life, non-contact, anti-interference ability. Therefore, in the complex and diversified circumstances between the electronic components of different machines and the physical processes standing at the basis of their functioning has determined the intensification of the research within the sensors field [3]. There are lots of literatures that deal with how to design and construct the special usage optoelectronic sensor, such as high-speed, temperature stability and high sensitivity [4].

The model of PD in optocoupling sensor, either numerical [5, 6] or analytic solutions [7] was researched. In order to achieve the fast, cheap sensor, the modern development of PD demands the simple process of modeling photodiodes components. One of the most frequently used ways, to fulfill that, is creating the equivalent electric model [8]. To evaluate the system performance, the transit time effect in the PD should be taken into account, so some high-speed PIN or Schottky-barrier photodiodes are essential [9]. But considering the cost, this is not reality for industrial applications. For this purpose, the optical sensitivity and coupling efficiency is very important, and the production process and the design model are often used since they are cost effective and easy to employ [10].

In this paper, the PD with the type of N_{well}-HVP_{well}-P_{sub} vertical structure is fabricated in the 1-poly-3-meatl BCD 0.35 μm technology [11]. A two-dimensional PD with a 200×400 μm^2 active area with each area is 20×20 μm^2. Test results for the response time of the PD model are described in the below sections.

In order to achieve the fast response speed and the stability of the sensor, the main blocks of the optoelectronic sensor should be researched in detailed.

2. Optocoupling Sensor Structure

In order to analyze the optocoupling sensor from the inner block diagram, Fig. 1 shows the geometric structure of the sensor and its corresponding application circuit. A signal source generated the pulse wave of different frequencies that serve as input signal I_{in}. When the photons incited the PD the photocurrent I_{ph} was generated [12]. To measure the dynamic response of I_{ph}, the photocurrent is amplified by a high bandwidth TIA (Transimpedance Amplifier) and was tested in the output of the structure [13].

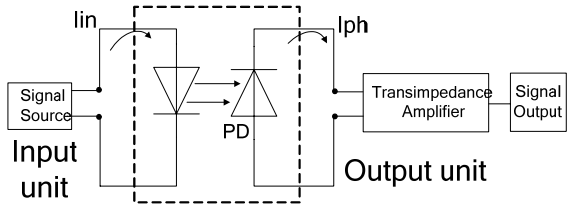

Fig. 1. Optocoupling sensor structure.

The response speed is the delay time from I_{in} to I_{ph} of the whole sensor and the stability with the variation of the temperature was determined by the structure of the PD. The gain of the sensor was controlled by the TIA circuit automatically. So the PD structure and the TIA circuit are the main point of this paper.

3. PD Model and TIA Circuit

3.1. PD Model

The PD was implemented by using a PN junction available in BCD technology between the N-well and the P-substrate [14]. Its basic structure is shown in Fig. 2, In the process of designing it, using the N_{well}-HVP_{well}-P_{sub} vertical structure, thereby reducing the substrate on the response speed of movement due to the diffusion of the light-generated carriers [15].

According to the maximum size of the detection diode, the design area of the PD is 200 μm×400 μm. Select 200 parallel light receiving array which width is 20 μm and length is 20 μm, too.

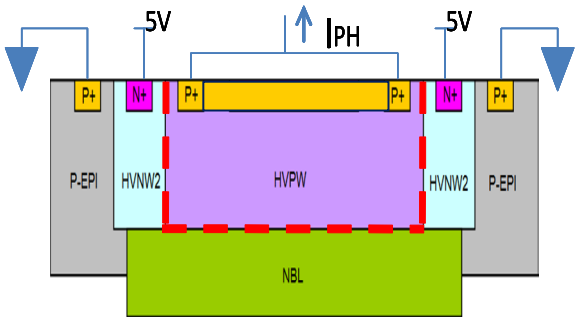

Fig. 2. PD structure.

When the photons go through the anti-reflection coating of the PD and incited electron-hole pairs, the I_{ph} was generated and it constructed by the $I_{diffuse}$ (diffusion current) and the I_{drift} (drift current) [16, 17], as showed in Fig. 3.

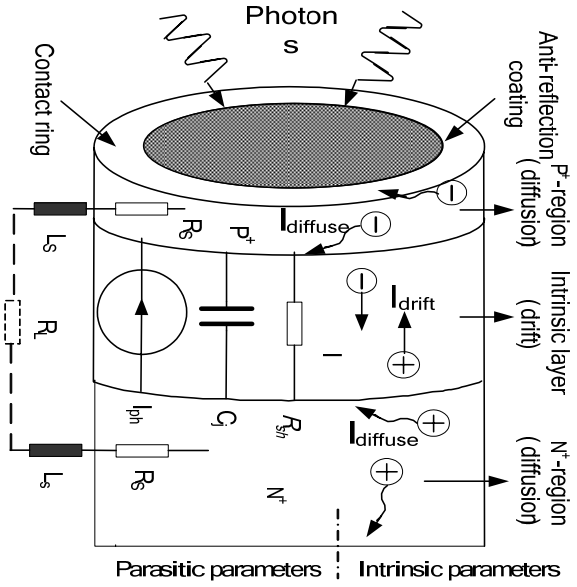

Fig. 3. PD equivalent structure.

Fig. 3 showed the PD includes the parasitic parameters and the intrinsic parameters. It can be equivalent to the following components and parameters. I_{ph} is the photocurrent generated by the incident radiation. C_j is the junction capacitance. R_{sh} is the shunt resistance and paralleled with the other components. R_s are the series resistance and series connected with all components in this model.

3.2. Response Time

The response speed of the sensor was mainly determined by the response time of the PD and TIA. For the novel structure was fabricated to the PD, the whole response time of the PD is controlled by the following three factors [18].

3.2.1. T_{RC}: Constant Time of Resistors and Capacitors

T_{RC} is determined by the C and the R, where R is the sum of the series resistance and the load resistance (R_s + R_L). C is the sum of the package capacitance and the photodiode junction capacitance. T_{RC} is given by:

$$T_{RC} = 2.2C(R_s + R_L), \quad (1)$$

3.2.2. $T_{diffuse}$: Diffusion Time

Carrier transit time may generate outside the depletion layer when incident light misses the PN junction and is absorbed by the surrounding area of the photodiode chip and the substrate section which is below the depletion area. The $T_{diffuse}$ required for these carriers to diffuse may sometimes be greater than several microseconds.

3.2.3. T_{drift}: Drift Time

Carrier drifts time can be calculated by formula 2, in which the v_d is transit speed and μ is the travelling rate. The E is the electric field. So the T_{drift} can be approximated as follows:

$$T_{drift} = d / v_d = d^2 / (\mu V_R), \quad (2)$$

From formula (1), (2), the response of the PD can be illustrated by the following equation:

$$T = \sqrt{T_{drift}^2 + T_{diffused}^2 + T_{RC}^2}, \quad (3)$$

Using the new structure of the PD, fewer carriers generated outside the depletion layer, C is small and the carrier transit time in the depletion layer is short. Therefore, these types are ideally suited for high-speed light detection. To decrease the response time of the PD, each of the factors mentioned above should be as small as possible.

3.3. TIA Circuit

The TIA has a high gain and wide bandwidth. The gain can be changed with the resistance step automatic. So the output V_O could not changed dramatically with the variation of the input signal. The circuit of TIA is showed in Fig. 4.

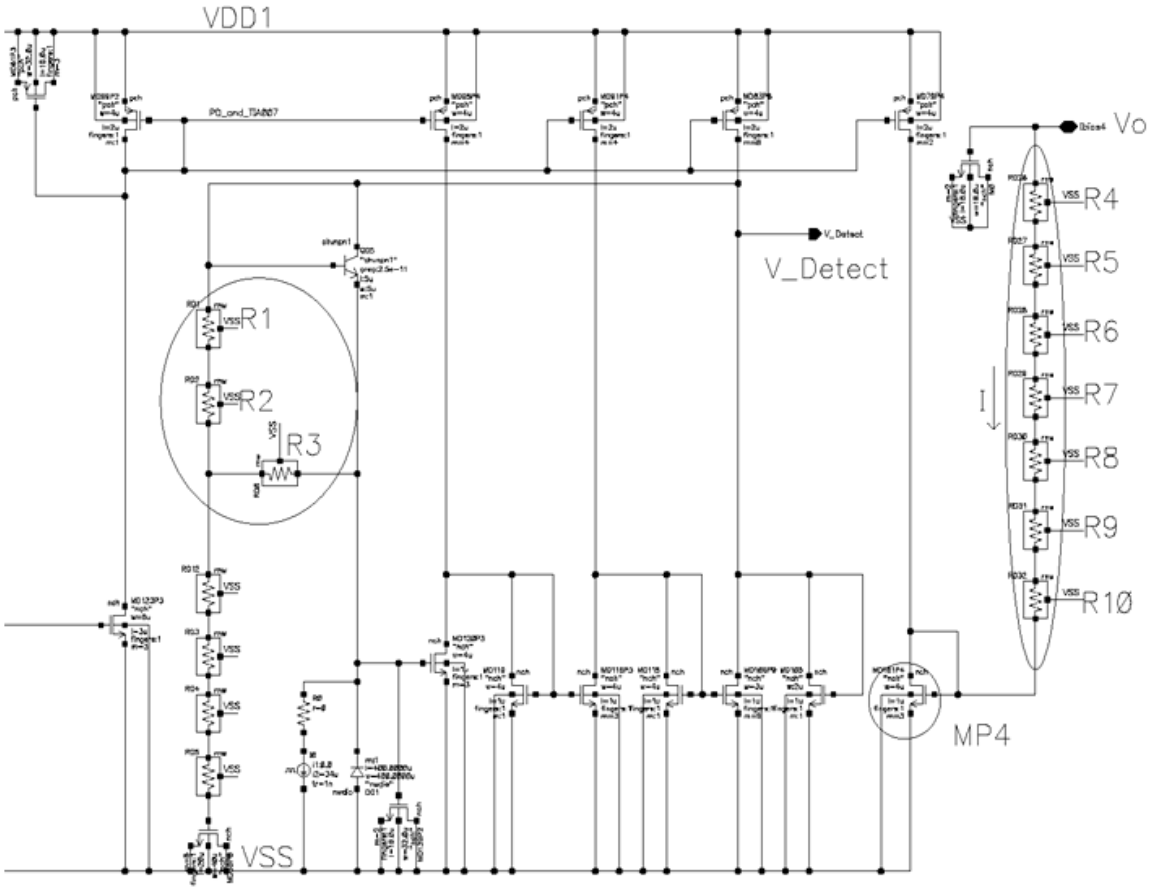

Fig. 4. PD and TIA circuit diagram.

In Fig. 4, the resistances of R1, R2, and R3 in series which length is 72 μm and width is 3 μm. Let the three same dimension shorting resistors as the option. When the square resistance (R□) is 1 kΩ then the value of R1 to R3 is 36 kΩ. In the non-adjustment cases, the gain of the transimpedance amplifier is 108 kΩ. Through shorting resistors or fusing metal wire, the range of the adjustable gain is 36 kΩ~216 kΩ and the step is 36 kΩ. The ratio of the range is 33.3 % to 200 % and the step is 33.3 %.

The MOS transistor (MP4) series the resistances (R4~R10) is used to generate the threshold voltage of the light detection module. The seven resistors in series which length is 17 μm and width are 5 μm. Also let the shorting resistors to be the Option. The R□ is 1 kΩ and then the value of R4 to R10 is 4.25 kΩ. The all resistances (RA) are 29.75 kΩ. The current (I) through the resistances is 10 μA, so the voltage on the resistances (Vo) is 0.3 V and the voltage on the MP4 is 1.05 V. So in the typical case, the $V_{-Detect}$ is 1.35 V. In the no lighting circumstances the $V_{-Detect}$ is 1.10 V. Through shorting resistor or fusing metal wire, the threshold voltage can be changed from 1.05 V to 1.475 V and the step is 42.5 mV.

Thus the TIA module can change the gain by the current which came from the PD module. Then the response time will be reduce. At the same time, according to the noise with the photocurrent to adjust the threshold voltage. So as to avoid amplify the noise in the preceding stage.

4. Simulation Results

4.1. Response time and Stability

According to formula (4), the I_{ph} can be calculated by the I_{in} while the power of the incident light P_{in} is 1.71 mW. When the λ is 840 nm, the optical sensitivity S was measured about 0.4 A/W. The range of the coupling efficiency Λ is 0.05~1.

$$I_{ph} = I_{in} \times \frac{P_{in}}{20mA} \times S \times \Lambda, \quad (4)$$

Using the Pspice simulation tool and VDD is 30 V. With the variation of the I_{in}, the I_{ph} can be set to 34 uA, and duty cycle is 4 %, the frequency is 25 kHz. Choose three temperatures such as -25 °C, 25 °C, and 100 °C to simulate the response speed and the temperature stability of the whole sensor.

Fig. 5 indicates the results of the whole sensor response speed. The yellow line represents I_{ph} and the red line is the output signal. When the working temperature varied from -25 °C ~ 100 °C, the simulation results showed that the sensor has good temperature ability and the response time changed a little when the temperature varied.

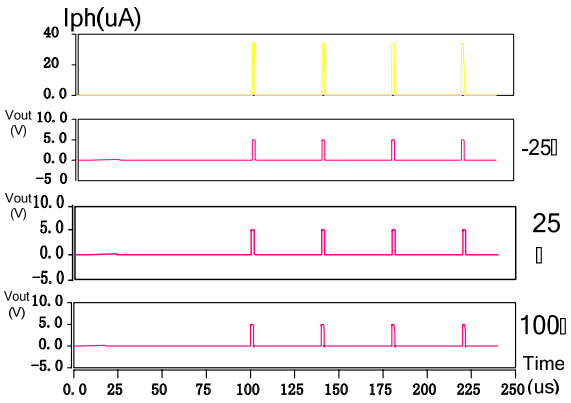

Fig. 5. Response time and stability.

In order to summarize the response time of the sensor and the blocks, the simulation was divided into two cases in the typical conditions. One is from the photon incited to the TIA (T_1) and the other is from the input port to the output port (T_2). Where the "R" indicates the delay time of the signal change from low-to-high and the "F" represents the delay time of the signal change from high-to-low. The simulated data is showed in Table 1.

Table 1. Response Time with Temperature Variations

T°C	T_{R1}	T_{F1}	T_{R2}	T_{F2}
-25	9.5 ns	38.4 ns	203.1 ns	157.2 ns
25	9.6 ns	41.5 ns	209.5 ns	153.0 ns
75	10.0 ns	40.2 ns	204.2 ns	157.8 ns
100	10.5 ns	38.7 ns	205.9 ns	151.1 ns
125	11.5 ns	38.5 ns	208.9 ns	156.8 ns

In the second case, when the temperature is 25°C, I_{ph} changed from the 5 uA~80 uA, simulated the influence of the current on T_R and T_F. The specific data is showed in Table 2.

Table 2. Response Time with Photocurrent Changes

I_{PD}(uA)	T_{R1}	T_{F1}	T_{R2}	T_{F2}
5	15.9 ns	34.7 ns	215.2 ns	187.9 ns
10	13.54 ns	39.9 ns	204.4 ns	150.1 ns
20	10.6 ns	41.5 ns	203.5 ns	153.0 ns
40	9.0 ns	42.7 ns	200.1 ns	150.1 ns
80	8.2 ns	43.5 ns	194.1 ns	147.2 ns

From the data of the simulation, it was showed that the response time of the PD is very short and it has the very good temperature coefficient.

4.2. Sensitivity of TIA

In order to shorten the response time, simulated the sensitivity of the TIA circuit. In the course of

simulation, the working temperature is -25 °C ~ 100 °C, the I_{ph} is 10 μA, and the rise time of I_{ph} is 100 us and then compared the output signal to get the response time of the TIA circuit.

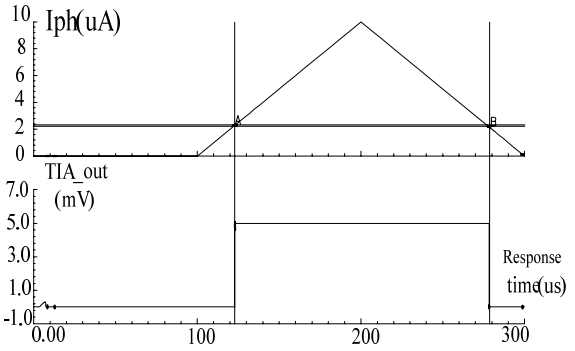

Fig. 6. Sensitivity of TIA.

From Fig. 6, when the I_{ph} rise up from 0 uA to 10 μA with the step is 0.01 μs; the response speed of the TIA is so fast. When the temperature is 25˚C, the response time of the rise time is 2.29 ns and the fall time is 2.17 ns.

5. Experimental results

The following two Figures illustrate the measurement results of the optoelectronic responses about the whole sensor. The yellow line corresponds to the I_{ph} and the red line represents to the output signal.

According with the formula 10, when the I_{in} is 6.2 mA, the I_{ph} is 10 uA and when the I_{in} is 12.4 mA, the I_{ph} is 20 uA. Set the R_L is 50 Ω and working temperature is 25˚C and the VDD is 30 V.

The transient response of the sensor was tested by a LeCroy 954 oscilloscope. While using the optcoupling sensor, the response speed and stability maybe influenced by different value of the photo current. In order to test the response time and stable of the designed optocoupling sensor, here, set two I_{ph} to test the response time. When the I_{ph} is 10 μA, the measurements of the response speed of the entire sensor were showed in Fig. 7.

Here, T_R is 205 ns and T_F is 153 ns. Compared the data between the Fig. 7 and the Table 2, it was showed that the measured data match the simulation data very well. When the I_{ph} is 20 μA, the response time was measured again, and the data was showed in Fig. 8.

Fig. 8 showed that the response time of the whole sensor will contain within the 208 ns and the 155 ns when the photo current varied from 10 μA to 20 μA.

Experimental results showed the response time could not change dramatically with the variable of the input signal. The test date matched the simulation data very well, and the sensor has a high speed and sensitivity characteristics.

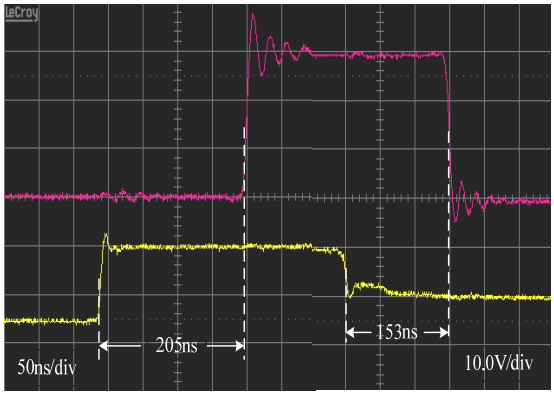

Fig. 7. Response time of the sensor: I_{ph}=10 μA.

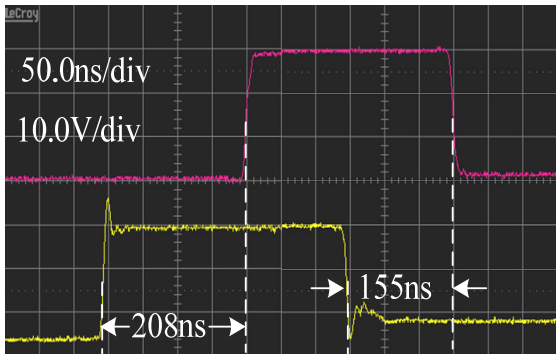

Fig. 8. Response time of the sensor: I_{ph}=20μA

6. Conclusions

This paper fabricates a novel PD structure in order to elevate the response speed of the optocoupling sensor. Based on 0.35 μm BCD technology designed and fabricated the sensor, which contains mostly N_{well}/P_{sub} structure of PD and TIA circuit analysis. It is verified that, the sensor has a good response speed and the temperature characteristics. With the working temperature range from -25˚C to 100˚C, when the I_{ph} is 10 uA, the maximum response time of the sensor is 205 ns. It can be seen clearly the PD and TIA can increase the response speed of the sensor and keep the good stability with the variation of the working temperature.

Acknowledgement

This work was partly supported by Key Lab of High-Speed Circuit Design and EMC, Ministry of Education, the Xidian University of China, and by a research grant from the National Natural Science Foundation (No. 61106026) of China.

References

[1]. P. Ciampolini, P. Mezzanotte, L. Roselli, R. Sorrentino, Accurate and efficient circuit simulation with lumped-element FDTD technique, *Microwave Theory and Techniques*, Vol. 44, Issue 12, 1996, pp. 2207-2215.

[2]. Chee Hing Tan, Shiyu Xisse, Jingjing Xie, Low noise avalanche photodiodes incorporating a 40 nm AlAsSb avalanche region, *IEEE Journal of Quantum Electronics*, Vol. 48, Issue 1, 2012, pp. 36-41.

[3]. I. M. Ciurus, M. Dimian, A. Graur, The analysis of the polaroid optocoupler mechanical-electrical sensor, *Advances in Electrical and Computer Engineering*, Vol. 10, Issue 4, 2010, pp. 29-34.

[4]. W. Feng, K. Mao, Design of smart temperature sensors system based on ART neural network, *Sensor and Transducers*, Vol. 154, Issue 7, July 2013, pp. 94-102.

[5]. J. M. Wiesenfeld, A. R. Chraplyvy, J. Stone, C. A. Burrus, Measurement of very-high-speed photodetectors with picosecond InGaAsP film lasers, *Electronics Letters*, Vol. 19, Issue 1, 1983, pp. 22-24.

[6]. M. Smiljanic, Z. Djuric, Z. Lazic, Electron transit time through depletion layer of GaInAs pn junction, *Electronics Letters*, Vol. 25, Issue 2, 1989, pp. 150-152.

[7]. Yao Yan, Chen, Hsiang-Yu, Huang, Jinsong, Yang Yang, Low voltage ands fast speed all-polymeric optocouplers, *Applied Physics Letters*, Vol. 90, Issue 5, 2007, pp. 053509-053509-3.

[8]. M. V. Lazovic, P. S. Matavulj, SPICE model of P-i-N photodiode for heaveside excitation, in *Proceedings of the EUROCON International Conference Computer as a Tool*, Vol. 1, 2005, pp. 875-878.

[9]. G. George, J. P. Krusius, Dynamic response of high-speed PIN and Schottky-barrier photodiode layers to nonuniform optical illumination, *Light Wave Technology*, Vol. 12, Issue 8, 1994, pp. 1387-1393.

[10]. Myung-Jae Lee, Holger Rücker, Woo-Young Choi, Effects of guard-ring structures on the performance of silicon avalanche photodetectors fabricated with standard CMOS technology, *IEEE Electron Device Letters*, Vol. 33, Issue 1, 2012, pp. 80-82.

[11]. P. M. Kulshrestha, R. S. Saxena, Analysis of crosstalk in HgCdTe based vertical photoconductive LWIR detector arrays, *Sensors & Transducers*, Vol. 154, Issue 7, July 2013, pp. 138-142.

[12]. Chee Hing Tan, Shiyu Xie, Jingjing Xie, Low noise avalanche photodiodes incorporating a 40 nm AlAsSb avalanche region, *IEEE Journal of Quantum Electronics*, Vol. 48, Issue 1, 2012, pp. 36-41.

[13]. Kang Yu-Zhuo, Mao Lu-Hong, Xiao Xin-Dong, Xie Sheng, Zhang Shi-Lin, Design and simulation of a novel CMOS superimposed photodetector, *Optoelectronics Letters*, Vol. 8, Issue 4, 2012, pp. 02549-0252.

[14]. P. Aubert, H. J. Oguey, R. Vuilleumier, Monolithic optical position encoder with on-chip photodiodes, *Solid-State Circuits*, Vol. 23, Issue 2, 1988, pp. 465-473.

[15]. T. Kneževic, T. Suligoj, A. Šakic, L. K. Nanver, Optimization of the perimeter doping of ultrashallow p+-n--n+ photodiodes, in *Proceedings of the 34th International Convention (MIPRO' 2011), 23-27 May 2011, Opatija, Croatia*, 2011, pp. 44-48.

[16]. Wei-Jean Liu, O. T.-C. Chen, Li-Kuo Dai, Ping-Kuo Weng, Kaung-Hsin Huang, Far-Wen Jih, A CMOS photodiode model, in *Proceedings of the 5th IEEE International: Behavioral Modeling and Simulation Conference, BMAS*, 2001, pp. 102-105.

[17]. J. Jang, M. Joung, B. Choi, S. Hong, S. Lee, Dynamic analysis and control design of optocoupler-isolated LLC series resonant converters with wide input and load variations, *IET Power Electronics*, Vol. 5, Issue 6, 2012, pp. 755-764.

[18]. M. Yamamoto, M. Kubo, K. Nakao, Si-OEIC with a built-in PIN-photodiode, Electron Devices, Vol. 42, Issue 1, 1995, pp. 58-63.